

Document downloaded from:

<http://hdl.handle.net/10251/213043>

This paper must be cited as:

Al-Mohammed, A.; Kareem, RS.; Dang, CN.; Martí Vargas, JR.; Hale, WM. (2022). Analytical model for predicting prestress transfer bond-related parameters of 18 mm prestressing strands. *Journal of Building Engineering*. 56:1-14.  
<https://doi.org/10.1016/j.jobe.2022.104709>



The final publication is available at

<https://doi.org/10.1016/j.jobe.2022.104709>

Copyright Elsevier

Additional Information

1                   **ANALYTICAL MODEL FOR PREDICTING PRESTRESS TRANSFER BOND-**  
2                   **RELATED PARAMETERS OF 18 MM PRESTRESSING STRANDS**

3  
4                   Ahmed Almohammedi<sup>1</sup>, Rahman S. Kareem<sup>1,2</sup>, Canh N. Dang<sup>3</sup>,  
5                   José R. Martí-Vargas<sup>4\*</sup>, and W. Micah Hale<sup>1</sup>

6  
7                   <sup>1</sup> Department of Civil Engineering, University of Arkansas, Fayetteville, AR 72701, USA

8                   <sup>2</sup> Department of Structure, Shatrah Technical Institute, Southern Technical University,  
9                   Shatrah, Dhi Qar, Iraq

10                   <sup>3</sup> Thornton Tomasetti, Ho Chi Minh City, Vietnam

11                   <sup>3</sup> Institute of Concrete Science and Technology (ICITECH), Universitat Politècnica de València,  
12                   4G, Camino de Vera s/n, 46022 Valencia, Spain

13  
14                   \* Corresponding author: Email: [jrmarti@cst.upv.es](mailto:jrmarti@cst.upv.es)

15  
16                   **ABSTRACT**

17                   The bond between prestressing strand and concrete is necessary for the composite-action of  
18                   the two materials. This study develops an analytical model to investigate the bond  
19                   performance of 18-mm prestressing strands. The model considers the concrete compressive  
20                   strength for both conventional and self-consolidating concrete. It is then used to determine  
21                   the short- (at prestress transfer) and the long-term (after all prestress losses) transfer length  
22                   and strand end slip. The predicted short-term transfer length and strand slip values were  
23                   validated with the experimental results obtained from several pretensioned concrete beams  
24                   and girders, which had various geometric configurations, concrete compressive strength, and  
25                   number of prestressing strands. The results showed that the model provided a reasonable  
26                   prediction of bond performance. From the analysis of the predicted long-term transfer length  
27                   and strand end slip values, the long-term transfer length is on average 33% longer than the  
28                   short-term transfer length, whereas the increase in strand end slip is on average 24% from the  
29                   short- to the long-term stage. Regardless of concrete compressive strength and concrete type  
30                   (conventional and self-consolidating concrete), both the ACI-318 and AASHTO LFRD codes  
31                   provided a conservative limit for the predicted long-term transfer length values.

32 **KEYWORDS**

33 pretensioned concrete; bond model; prestressing strand; 18-mm strand; transfer length; slip

34

35 **1. INTRODUCTION**

36 When compared to reinforced concrete, pretensioned concrete is one of the dominant

37 materials in long-span structures. The use of high or ultra-high strength prestressing strand is

38 the driving factor. The yield strength of those strands (Grade 1860, 2200, and 24000) is

39 assumed to be 90% of its ultimate strength ( $f_{pu}$ ) [1–3], and is about 4 or 5 times greater than

40 that of Grade 420 reinforcing bar. To fully utilize the high-strength capacity, the prestressing

41 strand is pretensioned before casting concrete. Once the concrete reaches the compressive

42 strength required for prestress transfer, the prestressing strand is released. The bond at the

43 interface of the prestressing strand and concrete is crucial for transferring the prestress force

44 from the strand to the surrounding concrete material. In terms of structural design, the strand

45 bond has a direct correlation to transfer length (or transmission length); a significant design

46 parameter at the prestress transfer state and ultimate limit state [4,5]. Strand bond is

47 comprised of three factors: adhesion, friction, and mechanical interlocking. Adhesion is a

48 form of chemical bond, formed on the surface of the prestressing strand during the setting of

49 fresh concrete. Friction is a form of bearing stress, also known as the Hoyer's effect [6],

50 which is generated by the lateral expansion of the prestressing strand at prestress transfer. The

51 mechanical interlock is also a form of bearing stress, but generated by the resistance of the

52 hardened concrete to the longitudinal movement of the prestressing strand. The latter two

53 components have a major contribution to the bond strength [7–9]. These bond components

54 are affected by several factors, which typically include concrete compressive strength at

55 prestress transfer, strand surface condition, and strand diameter [10–16]. A direct

56 measurement of strand bond, for example by attaching strain gauges to the prestressing strand  
57 surface, may be not feasible as the gauges can distort the bond phenomenon and also become  
58 damaged during concrete casting. An indirect method is to develop a strand bond model,  
59 which typically consists of a set of mathematical equations to represent the interaction  
60 between the prestressing strand and concrete. The bond model can be used to implement  
61 finite-element modeling [17–22]. An analytical investigation is an alternative technique  
62 which provides similar outcomes [23–29]. Typical results consist of transfer length, strand  
63 slip, bond stress distribution, and strand stress variation of the prestressing strand. In fact,  
64 transfer length and strand slip are the parameters of interest, since they can be experimentally  
65 measured by reliable techniques for validating the analytical model [7,30–32].

66 Within the transfer zone, the prestress force in the prestressing strand is assumed to be  
67 linearly transferred to the surrounding concrete. When the transfer stage ends, the length of  
68 the transfer zone is technically termed as the transfer length, which is depicted in Figure 1.

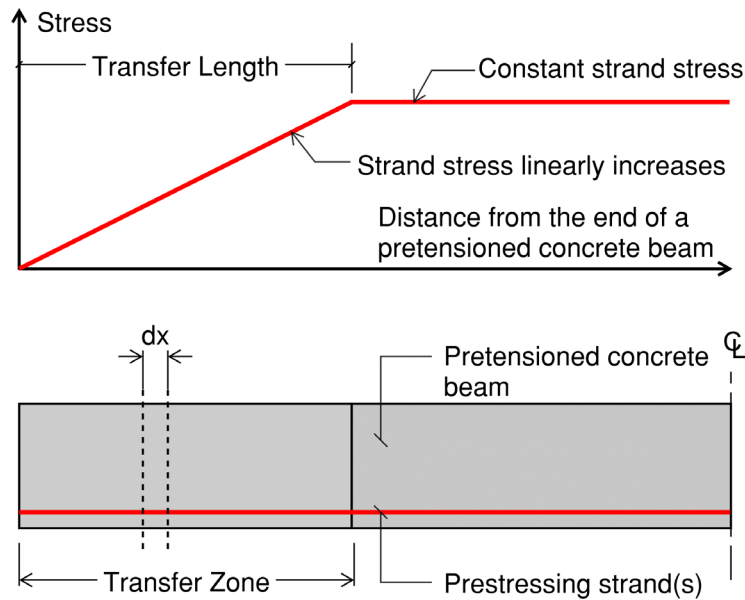
69 The significance of transfer length in the design of pretensioned concrete members is  
70 demonstrated through two aspects: (a) a short transfer length implies high compressive  
71 stresses and a risk of cracking at the member ends; and (b) a long transfer length negatively  
72 affects the shear strength and flexural capacity of the members. The ACI 318 [33] indicates  
73 that transfer length can be calculated using Eq. (1), which considers the effective stress ( $f_{se}$ )  
74 and strand diameter ( $d_b$ ) as the two key parameters in the prediction. This equation was  
75 developed based on an assumption of constant bond stress of 2.76 MPa (400 psi) [34].

76 Alternatively, transfer length can be simply estimated as  $50d_b$ . In a similar way, the AASHTO  
77 LRFD Bridge Design Specifications [35] also proposes the transfer length as  $60d_b$ .

78 
$$L_t = \frac{1}{20.7} f_{se} d_b \quad (f_{se} \text{ in MPa}) \quad (1)$$

79  $L_t = \frac{1}{3} f_{se} d_b$  ( $f_{se}$  in ksi)

80



81

82 Figure 1 - Transfer length and strand stress variation

83

84 Typical 7-wire prestressing steel strands, 13-mm and 15-mm nominal diameter, have been  
 85 used for pretensioned concrete applications for years. The use of 18-mm prestressing strand  
 86 has been only investigated recently. The prestress force provided by a 18-mm prestressing  
 87 strand is 38% and 93% greater than that provided by a 15-mm and 13-mm strand,  
 88 respectively. The use of the larger strands (18 mm) offers several advantages, such as  
 89 reducing the number of required strands and reducing girder depth and weight. The structural  
 90 efficiency of using 18-mm strands in bridge design and construction has been demonstrated  
 91 in a few projects in the U.S. [36,37]. However, the lack of the strand performance data and  
 92 the lack of design specifications have limited their use in the precast, prestressed concrete  
 93 industry. In fact, recent studies recommend further research to increase the database of  
 94 experimental results regarding the bond phenomena in self-consolidating concrete [15,16].

95 The research presented in this paper develops a strand bond model to predict transfer length  
96 and end slip for beams containing 18-mm prestressing strands cast in conventional or self-  
97 consolidating concrete. The experimental data from two testing methodologies have been  
98 used to validate and calibrate the proposed model: pullout forces from the North American  
99 Strand Producers (NASP) Bond Test —adopted by American Society for Testing Materials  
100 (ASTM) as Standard Test for Strand Bond (STSB) [38]— and the transfer length and strand  
101 slip measured in pretensioned concrete beams and girders.

102

## 103 **2. LITERATURE REVIEW**

104 Strand bond models have been developed throughout last two decades through extensive  
105 research efforts. Balazs's research [39] is one of the first studies focusing on developing a  
106 bond model for prestressing strand. The bond stress was considered to be a function of strand  
107 slip. Through solving a set of nonlinear equations, a closed-form solution of transfer length  
108 was achieved. However, two shortcomings exist: (a) the bond model was not based on any  
109 previous experimental investigation; and (b) no experimental data were presented for  
110 verification of the proposed transfer length equation. Den Uijl [40] refined the strand bond  
111 model by using the results of pull-out and push-in tests. The bond stress is a function of  
112 strand slip and variation of strand stress and strain. The model was then used to develop a  
113 transfer length equation. The lack of experimental verification for the predicted transfer  
114 length is a limitation of the study.

115 Park and Cho [41] developed a strand bond model and experimentally verified the model's  
116 applicability. The experimental study involved casting several 3-m long pretensioned  
117 concrete prisms with a cross section of either 120×120 mm or 150×150 mm. Each prism  
118 contained one 13-mm or 15-mm prestressing strand. The predicted transfer length was in a

119 good agreement with the test results for the investigated prestressing strands. Martí-Vargas *et*  
120 *al.* [42] further investigated the strand slip along the transmission and anchorage lengths of  
121 pretensioned concrete members using an analytical model. This model was derived from  
122 experimental research work, which involved measuring the strand end slip, the prestress  
123 force, and transmission and the anchorage lengths. A single 13-mm prestressing strand was  
124 embedded in the test specimens that had a cross-section of 100×100 mm. The model was  
125 assessed using theoretical equations and experimental results from the literature. The study  
126 proposed an analytical bond model to predict the slip distribution of 13-mm prestressing  
127 strands within the transfer length. In fact, these two studies have a similar shortcoming, in  
128 which the experimental verification was conducted on small-scale pretensioned concrete  
129 members or small-size prestressing strands.

130 Dang *et al.* [43] developed a model for 15-mm prestressing strand by using the test results of  
131 the Standard Test for Strand Bond (STSB) specified by ASTM A1081 [38]. The STSB is able  
132 to provide a reliable indication of the bond condition of prestressing strand [9]. The effect of  
133 concrete compressive strength was additionally considered in the strand bond model. These  
134 are two dominant factors affecting strand bond. As a result, the model provided a reasonable  
135 transfer-length prediction from an experimental database of 19 pretensioned concrete beams.  
136 These data were collected from similar studies of 45 beams cast at the University of  
137 Arkansas. The researchers found that the transfer length predicted by ACI 318 limit of  $50d_b$  is  
138 conservative if the concrete has compressive strength of 26.7 MPa (4 ksi) or greater at  
139 prestress transfer. Despite these findings, one main limitation is that the conclusion is only  
140 applicable for the transfer length at prestress transfer. To overcome the limitation, Kareem *et*  
141 *al.* [44] further refined the proposed model by considering the effect of concrete creep and  
142 shrinkage to the long-term performance of strand bond. It was analytically determined that

143 the transfer length of the prestressing strand can increase by 20% during the first 28 days of  
144 age, which is consistent with experimental study conducted by Barnes *et al.* [11]. On the  
145 other hand, it was observed that the transfer length can increase by 25% after one year of age  
146 and then remain nearly constant. Regardless of the specific findings for 15-mm prestressing  
147 strand, Kareem *et al.* [44] posts a concern about the effect of concrete creep and shrinkage to  
148 the long-term strand bond performance.

149 Regarding the bond performance of 18-mm prestressing strand, an important issue is that the  
150 diameter is 17% and 40% greater than 15-mm and 13-mm strands, respectively. As observed  
151 in Eq. (1), the strand diameter is considered a main parameter, which determines the strand  
152 perimeter in contact with the surrounding concrete. It should be noted that a greater strand  
153 diameter (and perimeter) improves bond performance linearly. However, if the prestress level  
154 introduced in the strands is the same, which typically corresponds to  $0.75f_{pu}$  as a maximum  
155 established in manuals and design codes, a greater strand diameter (and area) results in a  
156 worse bond condition [34]. As the area/perimeter ratios are 2.56, 2.18, and 1.88 for 18-mm,  
157 15-mm, and 13-mm prestressing strands, respectively, the worst bond condition and then the  
158 greater transfer length correspond to 18-mm prestressing strands, which present the higher  
159 area/perimeter ratio.

160

### 161 3. RESEARCH SIGNIFICANCE

162 A strand bond model is developed for 18-mm, Grade 1860 prestressing strand. The bond  
163 stress function is derived from the STSB data. A calibration factor is adopted to account for  
164 the difference in the bond mechanism between the pretensioned prestressing strand used in  
165 pretensioned concrete members and the non-pretensioned prestressing strand used in the  
166 STSB. The transfer length and strand slip are the parameters of interest derived from the



167 strand bond model. The database for verification included 24 pretensioned concrete beams  
168 cast with high-strength conventional concrete or self-consolidating concrete, and a number of  
169 medium to large-scale pretension concrete girders cast with a wide range of concrete  
170 strengths. The applications and limitations of the developed model are discussed at the end of  
171 the research.

172

#### 173 **4. ANALYTICAL APPROACH**

174 Equation (2) is the general form of the strand bond equation [43]. The bond stress  $u(x)$  at the  
175  $x$  location in the transfer zone is exponentially proportional to the strand slip  $s(x)$  through the  
176  $\alpha$  coefficient. The bond magnitude of the non-pretensioned prestressing strand is represented  
177 by  $u_f$ . The coefficient  $k_b$  represents a calibration coefficient, which is used to calibrate the  
178 difference in the bond mechanisms as discussed below.

$$179 \quad u(x) = k_b u_f \left[ \frac{s(x)}{s_f} \right]^\alpha \quad (2)$$

180 For pretensioned prestressing strand in a concrete member, Hoyer's effect and mechanical  
181 interlock simultaneously contribute to the bond magnitude as aforementioned. For the non-  
182 pretensioned prestressing strand in the STSB, the mechanical interlock is the only component  
183 contributing to the bond magnitude. Pozolo and Andrawes [45] proposed a calibration  
184 coefficient  $k_b$  of 1.9 for 13-mm prestressing strand. The finite element analysis performed for  
185 verification showed a strong correlation to the test results. Dang *et al.* [43] investigated the  
186 applicability of the coefficient proposed by Pozolo and Andrawes in the development of a  
187 bond model for 15-mm prestressing strand. The predicted transfer length was in agreement  
188 with the experimental data. From these findings, it was determined that the calibration  
189 coefficient can be independent from the diameter of prestressing strands. In this study, this

190 coefficient is adopted for 18-mm prestressing strand.

#### 191 **4.1. Standard Test for Strand Bond**

192 The STSB test procedure is presented in detail in ASTM A1081 [38]. Therefore, only a brief  
193 description is provided in this section. A non-pretensioned prestressing strand sample is cast  
194 in the center of a steel tube. The tube is 125-mm in diameter and 450-mm in length. A  
195 debonded region of 50 mm is provided near the base plate of the steel tube. Accordingly, the  
196 embedment length of the strand sample is 400 mm. The steel tube is filled with mortar—a  
197 mixture of sand, cement, and water, which has compressive strength in a range of 31.1 MPa  
198 to 34.5 MPa at the time the strand sample is tested. **The STSB is performed 24 plus/minus 2**  
199 **hours after casting** by applying a pullout force at one end and measuring strand slip at the  
200 other end. The pullout force corresponding to the initial strand end-slip of 0.25 mm ( $s_i$ ) is the  
201 initial pullout force ( $P_i$ ). The pullout force corresponding to the final strand end-slip of 2.5  
202 mm ( $s_f$ ) is the final pullout force ( $P_f$ ). The final pullout forces of six samples are averaged and  
203 reported as the STSB pullout force.

204 The exponential coefficient  $\alpha$  in Eq. (2) is derived from two data points of STSB as shown in  
205 Eq. (3): ( $s_i, u_i$ ) and ( $s_f, u_f$ ); where  $u_i$  and  $u_f$  are the bond stresses corresponding to the free-end  
206 slips of  $s_i$  and  $s_f$ , respectively. Since the bond stress is proportional to the strand pullout force,  
207 Eq. (3) can be re-written as shown in Eq. (4). Based on the investigation of a number of  
208 STSB tests, Dang *et al.* [43] determined that the average ratio of  $P_i$  to  $P_f$  is 0.7. Accordingly,  
209 the coefficient  $\alpha$  is equal to 0.155. On the other hand, Eq. (2) can be simplified as shown in  
210 Eq. (5), where  $F_b$  is termed as the bond magnitude given in Eq. (6).

$$211 \alpha = \frac{\ln(u_i/u_f)}{\ln(s_i/s_f)} \quad (3)$$

212 
$$\alpha = \frac{\ln(P_i/P_f)}{\ln(s_i/s_f)} \quad (4)$$

213 
$$u(x) = F_b \times s^\alpha(x) \quad (5)$$

214 
$$F_b = k_b \frac{u_f}{s_f^\alpha} \quad (6)$$

215 The final pullout force  $P_f$ , which is used to calculate the final bond stress  $u_f$ , is based on the  
 216 research conducted by Morcous and Tadros [46]. A total of 58 pullout tests were performed  
 217 following similar testing procedures to those of ASTM A1081 [38]. Along with the mortar  
 218 mixture as specified by the standard, concrete was additionally used for the tests. For the  
 219 mortar, the cube compressive strength varied from 31 MPa to 34.5 MPa at one-day of age.  
 220 For the concrete, the 1-day compressive strength ranged from 27.6 MPa to 69.0 MPa. The  
 221 test results indicated that the STSB pullout force is a function of concrete compressive  
 222 strength; the higher the concrete strength, the greater the pullout force.

223 **4.2. Development of bond model**

224 The stress distribution along an element length  $dx$  within the transfer zone is described in  
 225 Figure 2. The specified parameters are defined in the notation list. The force equilibrium  
 226 equations of the bond stress ( $u$ ) to the concrete stress ( $f_c$ ) and to the strand stress ( $f_s$ ) are  
 227 presented in Eqs. (7) and (8), respectively. The determination of strand slip, a relative  
 228 displacement between the strand and the concrete, is shown in Eq. (9). By differentiating Eq.  
 229 (9) and substituting Eqs. (7) and (8), the relationship of slip and bond stress at position  $x$  is  
 230 obtained as shown in Eq. (10). Eq. (11) is re-written from Eq. (10) by substituting Eq. (4) and  
 231 (5) that results in a second-order, nonlinear ordinary differential equation. Two boundary  
 232 conditions are required to solve Eq. (11) and consist of the strand slip  $s(x)$  and its derivative  
 233  $s'(x)$  equal to zero at the end of the transfer length. The Runge-Kutta method was  
 234 implemented to solve a second-order, nonlinear ordinary differential equation with a fine

235 iterative step of 1/500 for the accuracy of the solution. The main steps of the solving  
 236 procedure are briefly summarized in the flowchart shown in Figure 3.

237  $u(x)C_s dx + A_c df_c = 0$  (7)

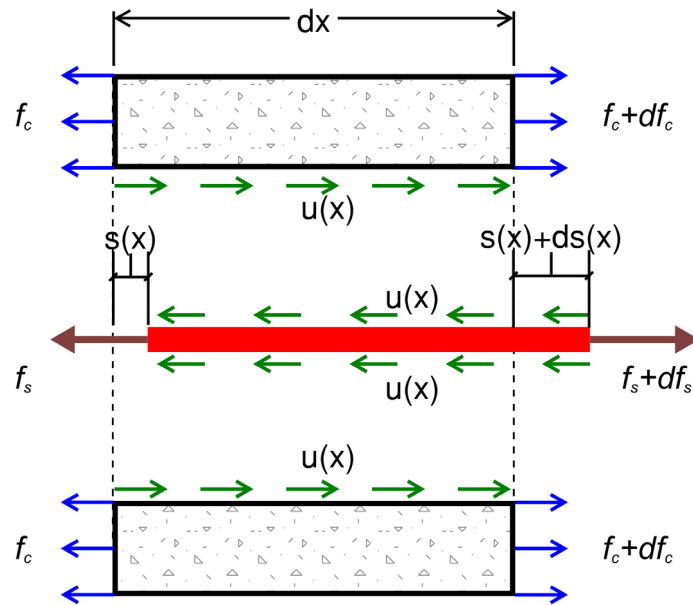
238  $-u(x)C_s dx + A_s df_s = 0$  (8)

239  $\frac{ds(x)}{dx} = \frac{df_s}{E_s} - \frac{df_c}{E_c}$  (9)

240  $\frac{d^2 s(x)}{dx^2} = \left( \frac{C_s}{E_s A_s} + \frac{C_s}{E_c A_c} \right) u(x)$  (10)

241  $s''(x) - \left( \frac{C_s}{E_s A_s} + \frac{C_s}{E_c A_c} \right) F_b \times s^\alpha(x) = 0$  (11)

242

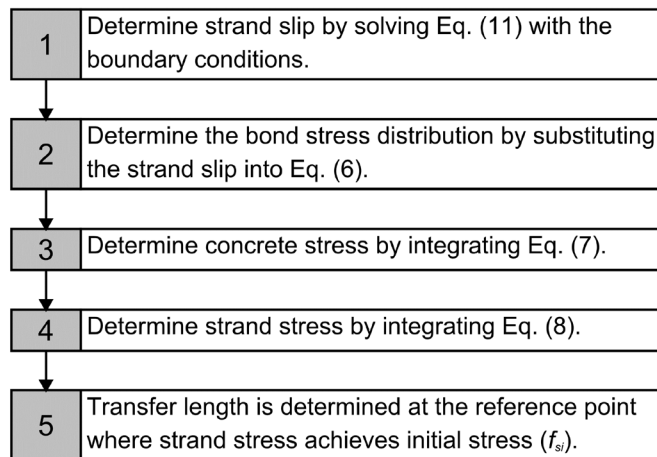


243

244 Figure 2 - Stresses distribution on element length  $dx$  (see  $dx$  position in Figure 1)

245

246



247

Figure 3 - Flowchart of transfer-length determination

248

249 To determine the short-term transfer length and bond-related parameters (i.e., strand end-slip  
250 and bond stress), the material properties at prestress transfer are used. These properties

251 include concrete compressive strength, concrete modulus of elasticity and initial strand stress.

252 At the long-term state, the long-term material properties are used, which include concrete

253 compressive strength at 28 days of age, concrete modulus of elasticity at 28 days of age and

254 effective strand stress after allowance for all prestress losses. Regarding the calibration

255 coefficient  $k_b$  introduced in Eq. (2), a value of 1.9 is used for the short-term predictions

256 whereas a value of 1.0 is used for the long-term predictions as discussed in Section 6.3.

257

## 258 5. EXPERIMENTAL DATA

259 The experimental data are collected from two sources; one from a research project at the

260 University of Arkansas, and the other one from the previous studies conducted at the

261 University of Nebraska–Lincoln, the University of Tennessee–Knoxville, and the University

262 of Texas–Austin.

## 263 5.1. University of Arkansas

264 The study involved casting twenty-four pretensioned concrete beams [47]. Four concrete  
265 mixtures were used to cast the beams as presented in Table 1. The mixtures were denoted by  
266 their type: N-CC for normal-strength conventional concrete, H-CC for high-strength  
267 conventional concrete, N-SCC for the normal-strength self-consolidating concrete, and H-  
268 SCC for high-strength self-consolidating concrete. The development of self-consolidating  
269 concrete complied with the thresholds required for precast prestressed concrete applications  
270 recommended by Khayat and Mitchell [48]. The compressive strength was tested using 100  
271 mm by 200 mm cylinders. The average concrete compressive strength ranged from 41.0 MPa  
272 to 65.0 MPa at prestress transfer (1 day of age) and 63.0 MPa to 92.0 MPa at 28 days of age.  
273 The pretensioned concrete beams had a cross-section of 165 mm by 305 mm and a length of  
274 5.4 m. All beams were cast with 18-mm, Grade 1860 prestressing strand. The prestressing  
275 strands were tensioned to  $0.75f_{pu}$  prior to casting. Sixteen beams were cast with one strand,  
276 and eight beams were cast with two strands. The reinforcement details for the two beam  
277 configurations are shown in Figure 4-(1) and Figure 4-(2).

278 Two pretensioned concrete beams were cast simultaneously using one concrete batch. The  
279 beams were cured in the wooden forms for approximately one day. The sides of the forms  
280 were then unfolded which allowed the research team to take measurements, as shown in  
281 Figure 5-(1). A set of target points (steel discs) were glued onto the surface of the beams at  
282 the level of the prestressing strand on both sides and at both ends of the beams as typically  
283 illustrated on Figure 4-(3) and Figure 5-(2). Concrete strains were measured using 200-mm  
284 long demountable mechanical strain gauges (DEMEC) as shown in Figure 5-(3). The initial  
285 (zero strain) readings were recorded before prestress release. After gradually releasing the  
286 prestressing strand, the concrete strains were recorded immediately. The beams were then

287 moved to a storage yard. The transfer length of the prestressing strand was determined from  
288 the measured concrete strain profile in combination with the 95% average maximum strain  
289 (AMS) method developed by Russell and Burns [49], which relies on the change in slope of  
290 the concrete strain profile. The distance from the member end (live or dead) to the point at  
291 which 95% average maximum strain is measured represents the corresponding transfer length  
292 of the prestressing strand.

293 A micrometer was used to measure strand slip at the end of prestressing strand through a  
294 metal clamp attached to the strand portion protruded from the beam ends, as typically  
295 illustrated in Figure 4-(3). The readings were taken at the same time concrete surface strains  
296 were measured. The nominal strand slip is the difference between the initial reading and the  
297 subsequent reading. The strand slip at prestress transfer was determined by subtracting the  
298 elastic shortening of the free strand portion from the nominal strand slip [50].

## 299 **5.2. Other Universities**

300 Tadros and Morcous [51] evaluated the transfer length of 18-mm prestressing strand in four  
301 prismatic specimens with different levels of reinforcing confinement. The prisms had a 178-  
302 mm square cross-section and were 2.4 m long. Self-consolidating concrete, which had a  
303 compressive strength of 41.4 MPa at release, was used to cast the prisms. One prestressing  
304 strand was placed at the center of each prism and tensioned to  $0.75f_{pu}$ . The measured transfer  
305 length at prestress transfer was 787 mm on average, which is 88% and 74% of the ACI 318  
306 ( $50d_b = 890$  mm) and AASHTO ( $60d_b = 1070$  mm) limits, respectively. The effect of  
307 confinement was minimal on the measured transfer length.

308 Patzlaff *et al.* [52] measured the transfer length of 18-mm prestressing strand in eight 8.53-m  
309 long T-girders. The girder section was 610 mm deep, 200 mm wide at the stem, and 810 mm  
310 wide at the top flange. Each girder contained six prestressing strands tensioned to  $0.75f_{pu}$ . All

311 girders were cast with self-consolidating concrete, which had a release-strength and 28-day  
 312 strength of 63.5 MPa and 78.5 MPa, respectively. The average transfer length measured at  
 313 prestress transfer was 527 mm. This transfer length is 59% and 49% in comparison to the  
 314 ACI 318 ( $50d_b = 890$  mm) and AASHTO ( $60d_b = 1070$  mm) limits, respectively. On the other  
 315 hand, similar to the observation on prism specimens [51], the confining reinforcement had no  
 316 significant effect on the measured transfer length.

317 Maguire *et al.* [53] measured the transfer length for two full-scale double-Tee girders. The  
 318 girder section was 502 mm deep, 2438 mm wide and 15.24 m long. High-strength self-  
 319 consolidating concrete was used for the girder fabrication. The concrete had a compressive  
 320 strength of 83 MPa release and 103 MPa at 28 days of age. Each stem of the girders  
 321 contained ten 18-mm prestressing strands tensioned to  $0.6f_{pu}$ . The average measured transfer  
 322 length at prestress transfer was 419 mm, which is significantly shorter than the ACI 318 ( $50d_b$   
 323 = 890 mm) and AASHTO ( $60d_b = 1070$  mm) limits.

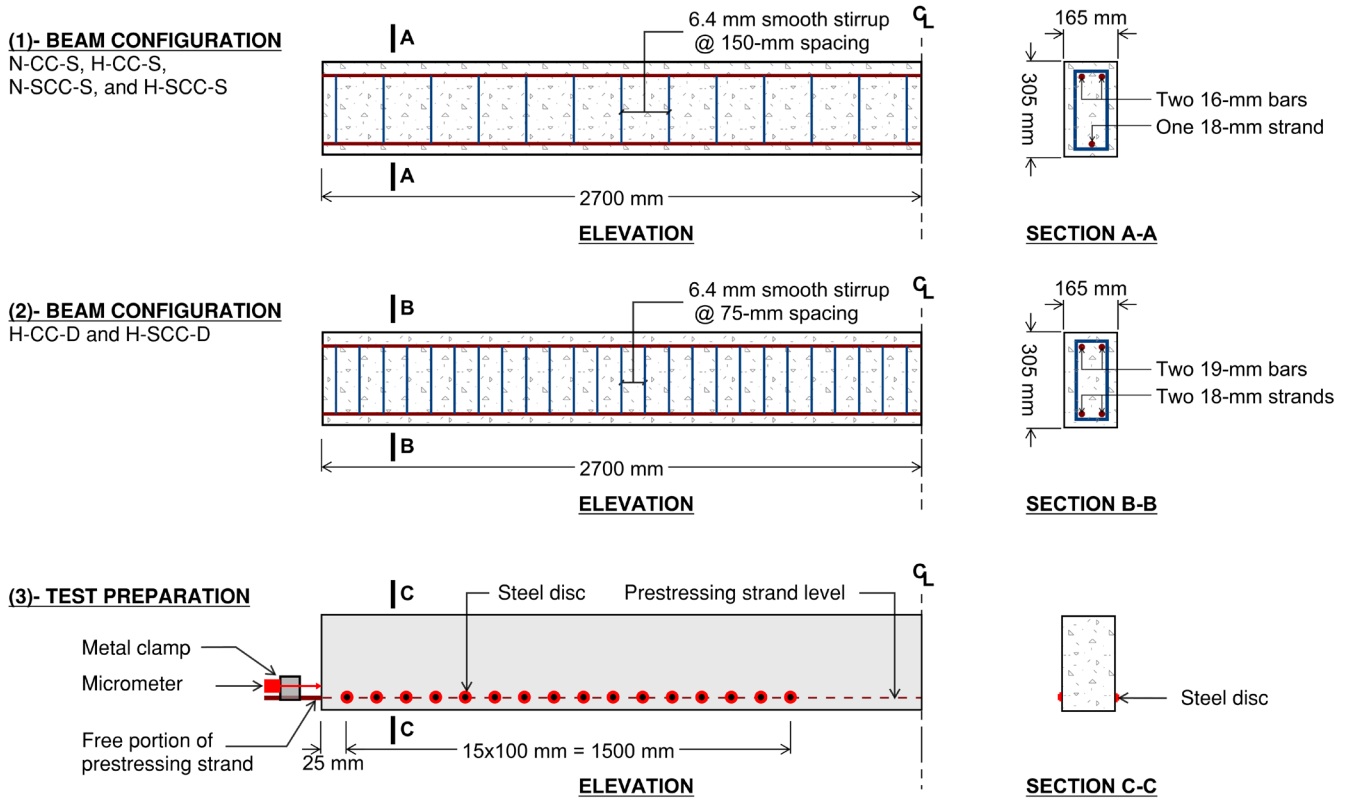
324

325 Table 1 - Concrete mixture proportions

Concrete mixture	N-CC	H-CC	N-SCC	H-SCC
Cement, kg/m <sup>3</sup>	415	415	460	489
Coarse aggregate, kg/m <sup>3</sup>	996	996	834	834
Fine aggregate, kg/m <sup>3</sup>	809	863	881	826
Water, kg/m <sup>3</sup>	166	145	184	196
Water / Cement ratio ( <i>w/cm</i> )	0.4	0.35	0.4	0.4
Slump flow, mm	N/A	N/A	660	640
Compressive strength at prestress transfer $f'_{ci}$ , MPa	43	63	41	54
Compressive strength at 28 days of age $f'_c$ , MPa	66	92	63	73
N-CC = normal-strength conventional concrete; H-CC = high-strength conventional concrete; N-SCC = normal-strength self-consolidating concrete; H-SCC = high-strength self-consolidating concrete.				

326

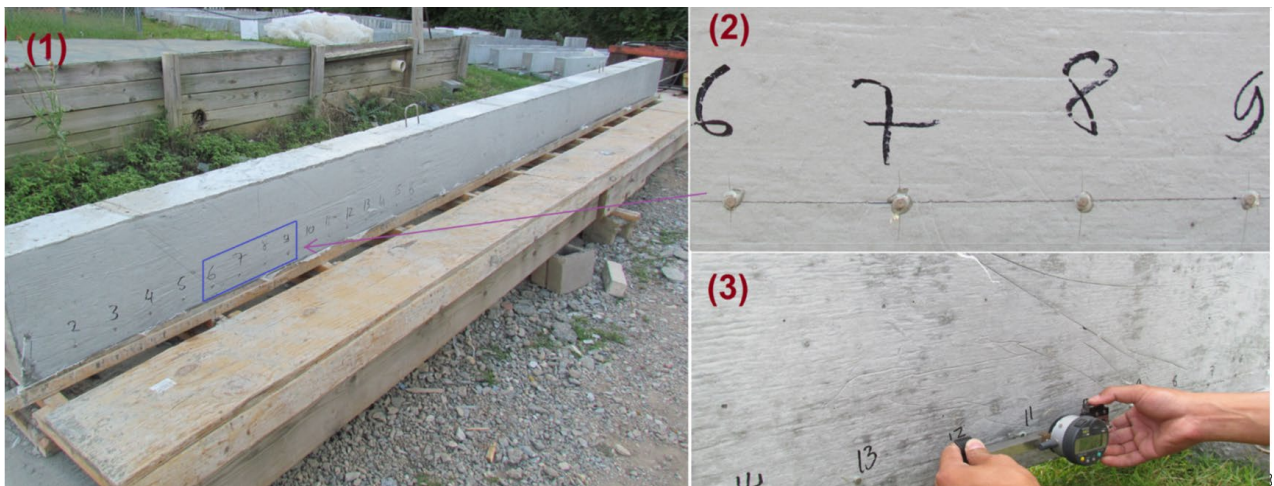




327

328 Figure 4 - Beam configurations and test setup for measurement of transfer length and strand  
329 slip

330



331

332 Figure 5 - Transfer length measurement: (1) attachment of target points on the surface of a  
333 pre-tensioned concrete beam after removing the form; (2) a set of target points placed at  
334 spacing of 100 mm; (3) use of mechanical strain gauge to record data

335

336 In related research, Song *et al.* [54] measured the transfer length and investigated the splitting  
337 force for two AASHTO Type I girders. Girder I was cast with 18-mm, Grade 1860  
338 prestressing strand. Girder II was cast with 16-mm, Grade 2270 prestressing strand. High-  
339 strength self-consolidating concrete was used for fabrication of both girders. The concrete  
340 compressive strength at release was approximately 67 MPa. Each girder contained 12  
341 prestressing strands tensioned to  $0.75f_{pu}$ . The measured transfer length of 18-mm prestressing  
342 strand at prestress transfer was 537 mm, which is 60% and 50% of the predicted values by  
343 ACI 318 ( $50d_b = 890$  mm) and AASHTO ( $60d_b = 1070$  mm) limits, respectively. In addition,  
344 the use of high-strength concrete was the key reason for the short transfer length in  
345 comparison to the code limits.

346 In another study, Morcouc *et al.* [36] measured the transfer length of prestressing strand in  
347 two NU 1350 girders. The first girder was 34.0 m long and contained twenty-four 18-mm  
348 prestressing strand. The second girder was 43.0 m long and contained thirty-seven  
349 prestressing strands. For both girders, the prestressing strands were tensioned to  $0.75f_{pu}$ . The  
350 self-consolidating concrete reached 51.5 MPa and 71.4 MPa at one day and at 28 days of age,  
351 respectively. On average, the measure transfer length at prestress transfer was 810 mm, which  
352 is 91% and 76% of the predicted values for ACI 318 ( $50d_b = 890$  mm) and AASHTO ( $60d_b =$   
353  $1070$  mm) limits, respectively.

354 Recently, Salazar *et al.* [55] investigated the structural behavior of the end-region for two  
355 Tx46 and two Tx70 girders. All girders were 9.0 m long. The Tx46-I and Tx46-II girders  
356 were 1168 mm deep and respectively contained twenty-four and thirty 18-mm prestressing  
357 strands. The concrete compressive strength at release was 39.3 MPa and 35.9 MPa for the  
358 first and second girder, respectively. The Tx70-I and Tx70-II were 1778 mm deep and  
359 contained twenty-eight and forty-two prestressing strands, respectively. The concrete

360 compressive strength at release was 44.9 MPa and 57.3 MPa, respectively. All prestressing  
361 strands were tensioned to  $0.75f_{pu}$ . The measured transfer lengths at prestress transfer were  
362 1062 mm, 814 mm, 914 mm, and 960 mm for the Tx46-I, Tx46-II, Tx70-I, and Tx70-II,  
363 respectively. In comparison to the code-predicted values, the measured transfer lengths were  
364 partially longer than the ACI 318 ( $50d_b = 890$  mm) and less than the AASHTO ( $60d_b = 1070$   
365 mm) limits.

366 It should be noted that the end zones of the girders tested by Morcous *et al.* [36] and Salazar  
367 *et al.* [55] experienced cracking along the web and bottom flange during the prestress transfer  
368 stage.

369 As in this study, it is noteworthy that transfer lengths were determined by applying the 95%  
370 average maximum strain (AMS) method developed by Russell and Burns [49]. The  
371 experimental data were obtained from DEMEC strain gauges at 100 mm spacing  
372 [36,51,53,54] or at 50 mm spacing [52], and from electrical strain gauges installed on the  
373 strands at 150-300 mm [55] which required a modified version of the 95% AMS method.

374

## 375 **6. ANALYSIS AND DISCUSSIONS**

### 376 **6.1. Transfer Length Verification**

377 Figure 6 presents the measured transfer lengths at prestress transfer for the twenty-four  
378 pretensioned concrete beams tested at University of Arkansas. The predicted values of  
379 transfer length at prestress transfer (short-term) and after allowing for all prestress losses  
380 (long-term), which were accounted for by considering a final effective stress of  $0.75f_{si}$ , are  
381 also included, together with the limits from code provisions for transfer length. As it can be  
382 observed, the ACI 318 and AASHTO limits provide a conservative prediction for the transfer  
383 length (short- and long-term) from the perspective of the Ultimate Limit State design. On

384 average, the measured transfer length is 71% and 59% of the ACI 318 and AASHTO limits,  
385 respectively. Eq. (1) provides a prediction similar to AASHTO. The overestimation of the  
386 code equations comes from two sources: (a) the code equations ignore the contribution of  
387 concrete strength; and (b) the prestressing strands exhibit good bond. It is worth noting that  
388 the analytical method considers both factors that improve the transfer-length prediction: on  
389 average, the measured transfer length at prestress transfer is 98% of the predicted values.  
390 The comparison to the previous studies from other universities revealed two different  
391 observations. The analytical method provides a good prediction for the measured transfer  
392 lengths at prestress transfer sourced from Tadros and Morcouc [51], Patzlaff *et al.* [52],  
393 Maguire *et al.* [53], and Song *et al.* [54]. The measured transfer lengths are 103%, 92%, 87%,  
394 and 97% of the predicted values; assuming that the 3% exceeded in the first comparison is  
395 acceptable. On the other hand, the analytical method underestimates the measured transfer  
396 lengths of the pretensioned concrete girders investigated by Morcouc *et al.* [36] and Salazar  
397 *et al.* [55]. The measured transfer lengths are 123% and 128% of the predicted values. This  
398 difference is most likely due to the cracking in the end zones which was previously  
399 mentioned.

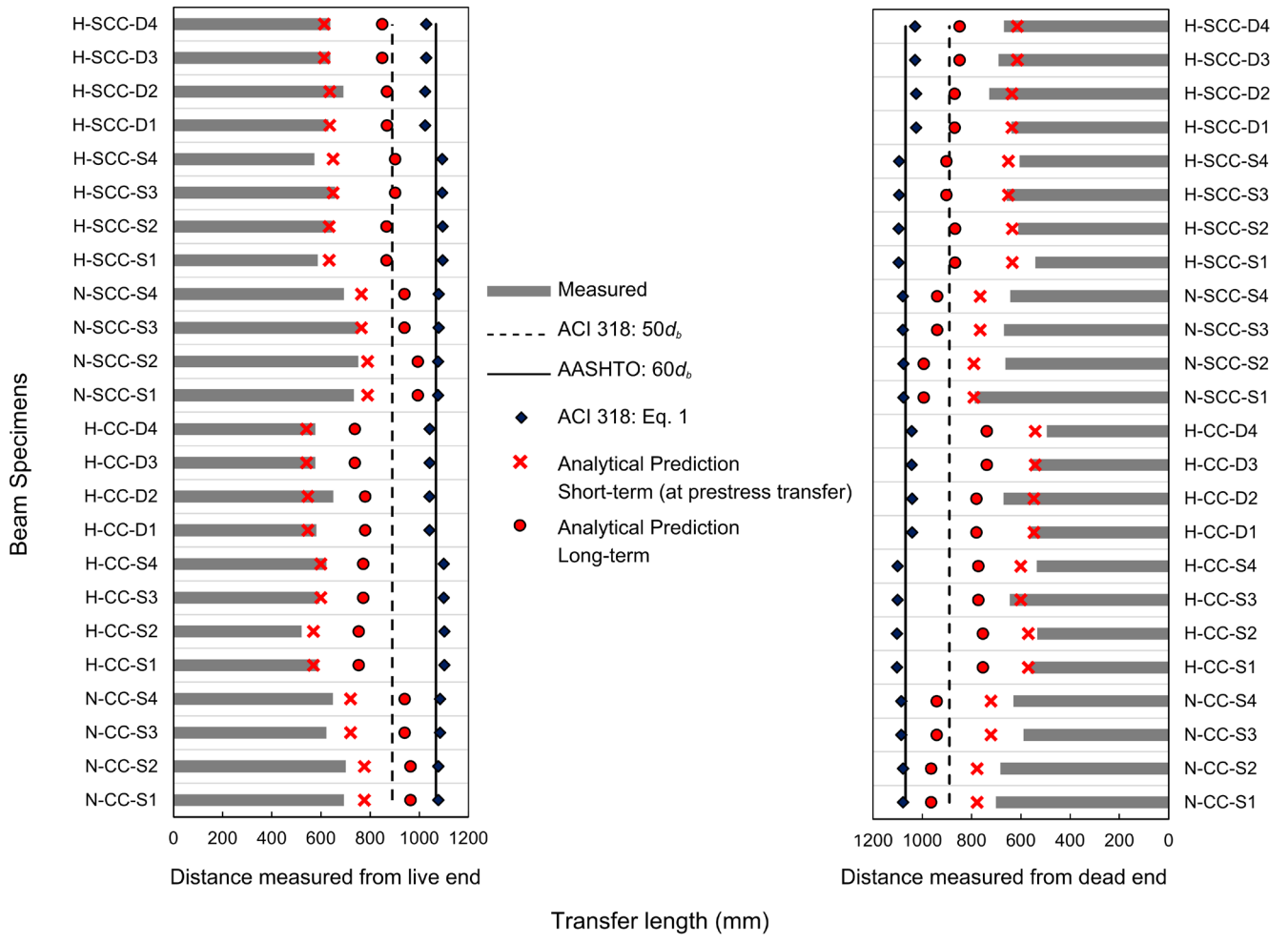


Figure 6 - Measured, analytical, and code-limit transfer lengths

**6.2. Strand Slip Verification**

Figure 7 presents the measured strand end slips at prestress transfer for the twenty-four pretensioned concrete beams tested at University of Arkansas. The predicted values of strand end slip at both short- and long-term stages are also included. In general terms, it can be observed that the measured and predicted short-term strand slip values ranged from 1.4 mm to 2.2 mm and 1.6 mm to 2.3 mm, respectively. The analytical bond model is able to capture this trend and provides a reasonable prediction for the experimental data. On average, the measured strand slip is 94% of the predicted values. This result ascertains that the strand slip

411 is dependent on the concrete compressive strength.

412

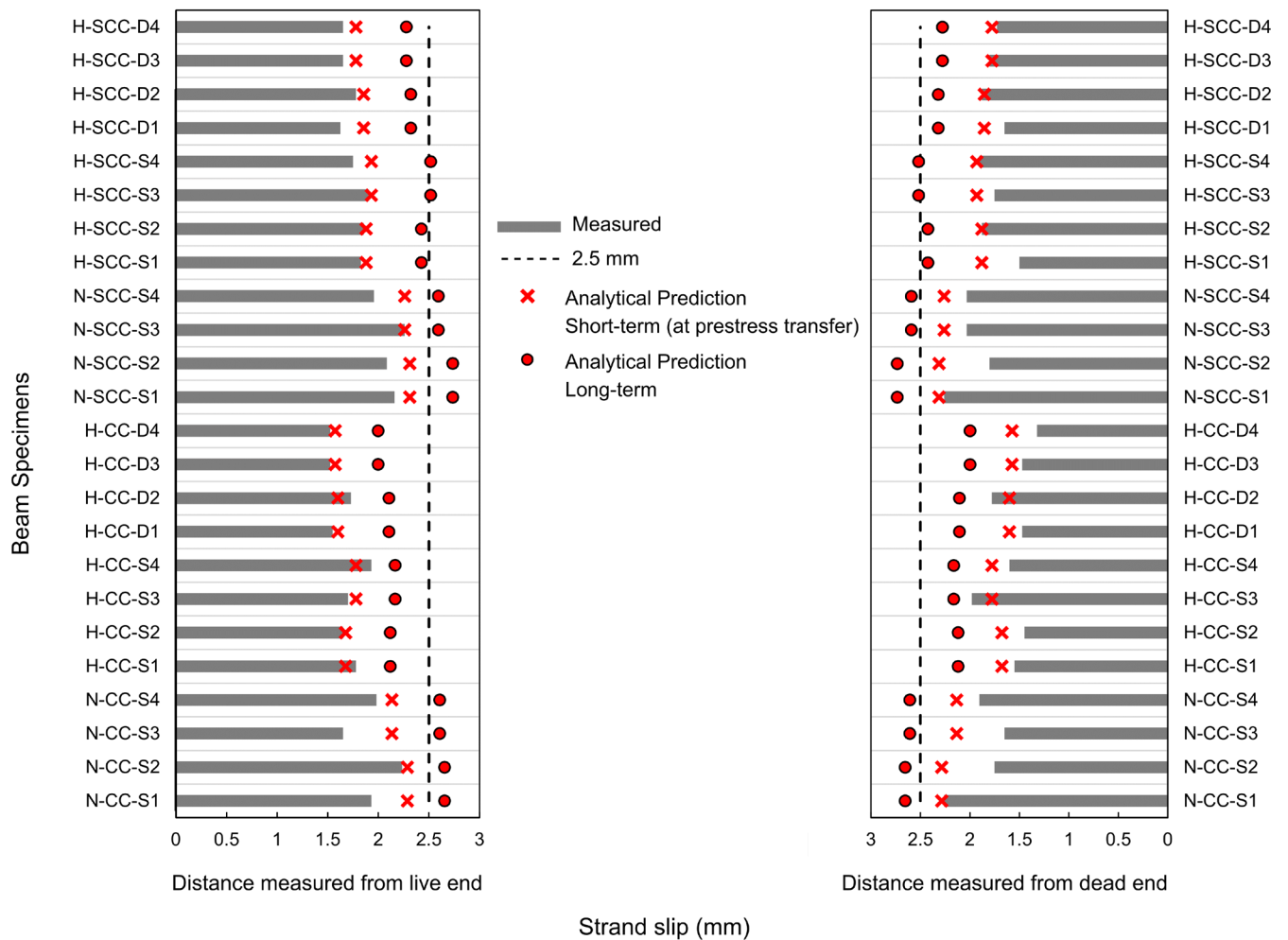


Figure 7 - Measured, analytical, and recommended threshold strand slip

The ACI 318 and AASHTO codes have no threshold for the strand slip even though several studies have demonstrated strand slip is a reliable indicator of strand bond [12,27,56]. Dang *et al.* [56] recommended a strand slip threshold of 2.5 mm based on the correlation of the strand end slip to the transfer and development length of prestressing strand. If a prestressing strand has slip at prestress transfer longer than 2.5 mm, the transfer length and development length is likely to be longer than the code limits; where development length is the required

422 length for prestressing strands to develop  $f_{ps}$ ; where  $f_{ps}$  is the stress in the prestressing steel  
423 strand at the time for which the nominal flexural capacity of a member is required [33,57].  
424 Therefore, the analytical determination of the strand end slip at the prestress transfer can  
425 provide an early indication of the transfer and development length of prestressing strands.  
426 This could then prevent a time-consuming and possibly costly experimental investigation.

### 427 **6.3. Bond Stress Distribution**

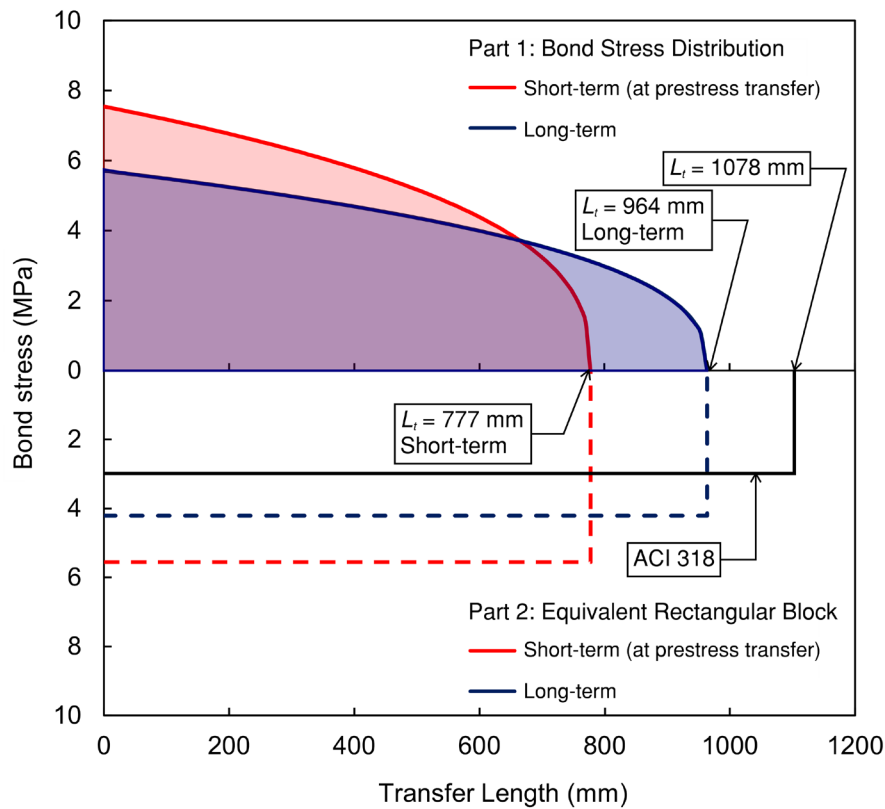
428 Figure 8 shows the bond stress distribution of beam specimen N-CC-S1. Part 1 at the upper  
429 portion of the graph presents the bond stress distribution in a nonlinear form. The bond stress  
430 is at a maximum at the beginning and reduces toward the end of the transfer zone. At this  
431 point the prestressing strand fully transfers the prestress force to concrete. Part 2 at the lower  
432 portion of the graph presents the equivalent bond stress, which is uniform in the transfer  
433 zone. The bond magnitude is determined by integrating the bond stress distribution in Part 1  
434 and then dividing by the associated transfer length.

435 Part 1 of Figure 8 presents the short- and long-term bond stress distribution. At this stage,  
436 Hoyer's effect and mechanical interlock (i.e., calibration coefficient  $k_b$  of 1.9 as  
437 aforementioned) contribute to strand bond. The predicted transfer length is 777 mm. For the  
438 long-term determination, under the effect of concrete creep and shrinkage in the transverse  
439 direction, the concrete adjacent to the prestressing strand deforms as it is subjected to the  
440 compressive stresses generated by the lateral expansion of prestressing strand [44]. Therefore,  
441 the contribution of Hoyer's effect is assumed minimal whereas the mechanical interlock  
442 becomes the main contributor to strand bond (i.e., calibration coefficient  $k_b$  reduces to 1.0).  
443 Simultaneously, the pretensioned concrete member experiences longitudinal deformation due  
444 to concrete creep and shrinkage which results in prestress losses. Additional degradation or  
445 deterioration of the pretensioned concrete members which may occur can also affect the bond

446 between the prestressing strand and concrete (e.g. strand corrosion). As a result, the  
447 magnitude of the maximum bond stress at the beginning of the transfer zone decreases with  
448 time, but the transfer zone increases. The predicted transfer length at this stage (long-term,  
449 without degradation/deterioration) of the beam specimen N-CC-S1 is 964 mm, which is 24%  
450 longer than the predicted value at the prestress transfer stage. For all beam specimens, the  
451 increase in transfer length ranged from 23% to 43% with an average of 33% as presented in  
452 Figure 6. This range is greater than the increase observed in the 13-mm and 15-mm  
453 prestressing strands, which typically ranges from 10%-20% [11,58]. The result shown in  
454 Figure 6 also indicates the ACI 318 limit of  $50d_b$  is not conservative in predicting the long-  
455 term transfer length. This finding reveals that the limit of  $50d_b$  is conservative for predicting  
456 the transfer length at prestress transfer, but not necessarily for the long-term transfer length.  
457 On the other hand, the ACI 318's Eq. (1) and AASHTO limit of  $60d_b$  provide a conservative  
458 prediction.

459 As shown in Part 2 of Figure 8, the equivalent bond stress at the short- and long-term is 5.56  
460 MPa and 4.21 MPa. The ACI 318 bond stress (2.76 MPa or 400 psi) is less than the  
461 equivalent bond stresses. This is the source for the conservative prediction of Eq. (1) for the  
462 short-term transfer length as shown in Figure 6. In terms of applications, determination of the  
463 equivalent bond stress is beneficial in finite-element modeling of pretensioned concrete  
464 members. If the location of interest is beyond the transfer zone, the equivalent bond stress can  
465 be used to reduce the computational effort. This is the case when calculating the ultimate  
466 flexural load capacity of pretensioned concrete members, when the location of interest is  
467 typically at the mid-span of the members [59–61]. Otherwise, if the location of interest is  
468 within the transfer zone, it is needed to accurately simulate bond stress distribution.





469

470 Figure 8 - Bond stress distribution along the transfer length of beam specimen N-CC-S1

471

#### 472 6.4. Strand Slip Distribution

473 Research commonly focuses on measuring strand end slip immediately after prestress

474 transfer. It is known that strand slip is a maximum at the free end and decreases as one moves

475 closer toward the end of the transfer zone. It is noteworthy that by having a better

476 understanding of the strand slip distribution in that region, one has a better understanding of

477 the behavior of prestressing strand in the transfer zone. Figure 9 presents the slip distribution

478 of beam specimen N-CC-S1. The slip distribution of the strand is nonlinear in the transfer

479 zone. For verification purpose, the slip distribution along the short-term transfer length was

480 compared to the one proposed by Martí-Vargas *et al.* [42] as expressed in Eq. (12), which was

481 obtained from an experimental basis, where  $s(x)$  is the strand slip at location  $x$  from the free

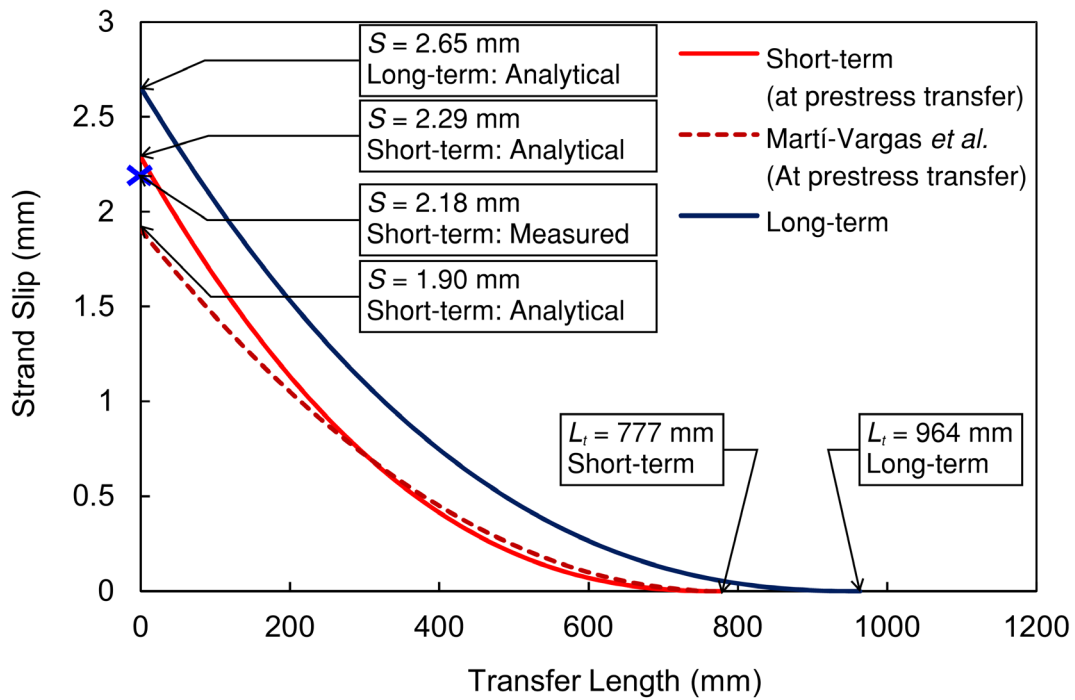
482 end of the pretensioned member.

$$483 \quad s(x) = 8.7 \frac{(L_t - x)^2}{L_t^2 \sqrt{f_{ci}}} \quad (12)$$

484 As observed in Figure 9, both distribution curves are generally in agreement, regardless of a  
 485 slight difference at the beginning of the transfer zone. The analytical method developed in  
 486 this study provides a closer prediction to the experimental data. In comparison to the  
 487 experimental results, the variation in the strand slip predictions is +0.11 mm in this study and  
 488 -0.28 mm for Martí-Vargas *et al.* [42]. In fact, it is worth mentioning that Martí-Vargas *et al.*  
 489 [42] studied the slip distribution of 13-mm prestressing strand. Therefore, based on ACI 318  
 490 [33] and AASHTO [35] provisions —transfer length is linearly proportional to strand  
 491 diameter— and the Guyon’s theory [42] —transfer length is linearly proportional to strand end  
 492 slip—, a ratio of strand diameters (18-mm/13-mm=1.4) was applied for consistent  
 493 comparison.

494 The results shown in Figure 9 indicated that strand slip increases over time. In comparison to  
 495 the short-term strand slip, the long-term strand slip of beam specimen N-CC-S1 increases  
 496 0.47 mm, which is 20.5% of the short-term slip. Similar to the increase observed in the  
 497 transfer length, concrete creep and shrinkage are the two dominant contributors. For all beam  
 498 specimens, the increase ranged from 15% to 32% with an average of 24% as presented in  
 499 Figure 7. This finding confirms the assumption of the minimal contribution of the adhesion to  
 500 strand bond as aforementioned. The prestressing strand in the transfer zone tends to slip  
 501 gradually over time, therefore any adhesion bond formed between the two materials would be  
 502 broken or fractured.

503



504

505 Figure 9 - Strand slip distribution along the transfer length of beam specimen N-CC-1

506

507 **6.5. Strand Stress Variation**

508 The variation of strand stress is presented in Figure 10. Due to the nonlinear distribution of  
 509 the strand bond (refer to Figure 8), the strand stress varies nonlinearly in the transfer zone.

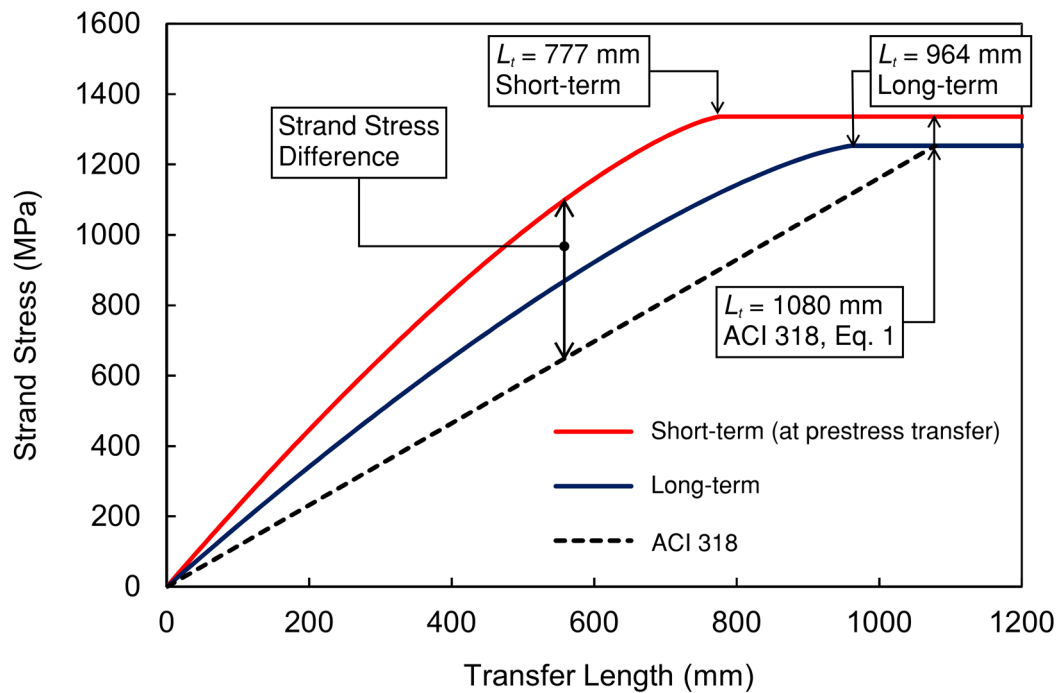
510 However, ACI 318 assumes a linear strand stress as shown in Figure 1. This assumption has  
 511 two implications. First, at a given location within the transfer zone, the strand stress is greater  
 512 than the assumed value as denoted by the “Strand Stress Difference” in Figure 10. In other  
 513 words, the prestress force transferred to the concrete is greater than the code-predicted value.

514 This could potentially lead to concrete cracking in the transfer zone. Second, the interaction  
 515 between multiple prestressing strands in the transverse direction is more severe. As

516 graphically visualized by Dang *et al.* [62], each prestressing strand has a ‘cylindrical transfer  
 517 zone’ to transfer the prestress force to the adjacent concrete. When several 18-mm

518 prestressing strands are placed in a grid pattern, the cylindrical transfer zones of these strands

519 are partially overlapped near the beginning of the transfer zone. The tensile stress is greater in  
 520 the overlapped regions and results in concrete cracking if the tensile stress is greater than the  
 521 concrete tensile strength. In fact, a linear strand stress variation was assumed by Dang *et al.*  
 522 to investigate the intensified tensile stress in the overlapped region. When considering the  
 523 nonlinear strand stress variation observed in this study, the extension of the overlapped region  
 524 is greater than expected, which increases the concrete region prone to cracking. This is likely  
 525 to be another factor for the long transfer length observed in Morcoux *et al.* [36] and Salazar *et*  
 526 *al.* [55] studies, where the prestressing strands were placed at a grid pattern of 51x51 mm.  
 527



528  
 529 Figure 10 - Strand stress variation along the transfer length of beam specimen N-CC-1  
 530

531 **6.6. Research Limitations**

532 The developed bond model excluded the effect of transverse reinforcement to the transfer  
 533 length of prestressing strands. Generally it is understood that transverse reinforcement can

534 provide a confining effect to the concrete in compression. Warenycia *et al.* [63] analytically  
535 quantified the contribution of transverse reinforcement in confining the concrete in the  
536 transfer zone which shortens the transfer length of prestressing strand. In fact, Maguire [51]  
537 and Patzlaff *et al.* [52] experimentally found minimal to no contribution of transverse  
538 reinforcement as mentioned in the previous discussions. Additional research is needed,  
539 particularly in testing large-scale pretensioned concrete girders, to fully understanding the  
540 effect of transverse reinforcement. Additionally, more experimental data (i.e., long-term  
541 transfer length and strand end-slip) are required and could be valuable to validate the  
542 proposed model in this study.

543

## 544 7. CONCLUSIONS

545 The following conclusions can be made based on the investigation on the strand bond of 18-  
546 mm prestressing strand:

- 547 • An analytical bond model has been developed for 18-mm prestressing strand.  
548 Through utilization of STSB results, the model considers the effect of concrete  
549 compressive strength on the bond performance. A coefficient of 1.9 is suitable for  
550 calibrating the difference in the bond mechanism of pretensioned and non-  
551 pretensioned 18-mm prestressing strands.
- 552 • The assumption regarding a minimal contribution of the adhesion to the strand bond  
553 in the transfer zone has been confirmed. The prestressing strand tends to slip  
554 gradually over time, so any kind of bond by adhesion formed between prestressing  
555 strand and concrete would be fractured.
- 556 • The developed analytical model provides a good prediction for the transfer length  
557 measured in pretensioned concrete beams. The measured transfer length is 98% of the

558 value predicted by the analytical model. For medium-scale pretensioned concrete  
559 girders, the analytical model can provide a reasonable prediction. However, the model  
560 underestimates the transfer length of large-scale pretensioned concrete girders due to  
561 cracking in the transfer zone.

562 • Transfer length increases over time. The long-term transfer length is 33% longer than  
563 the short-term. The ACI 318 Eq. (1) and AASHTO limit ( $60d_b$ ) adequately predict the  
564 short- and long-term transfer lengths. The ACI 318 limit of  $50d_b$  is conservative for  
565 predicting the short-term transfer length but not necessarily conservative for the long-  
566 term transfer length.

567 • The bond stress distribution is nonlinear in the transfer zone. In comparison to the  
568 short-term bond stress distribution, the maximum long-term bond stress is decreased,  
569 but the extension of the transfer zone is increased.

570 • The short-term strand slip is reasonably predicted by the analytical model. The  
571 measured strand slip is 94% of the predicted values. In comparison to the short-term  
572 strand slip, the long-term strand slip is 24% greater on average.

573 • The strand slip distribution is nonlinear in the transfer zone. The slip is maximum at  
574 the beginning of the transfer zone (free end of the member) and reduces toward the  
575 end of the transfer zone. The variation of the short- and long-term strand slip is  
576 similar.

577 • The strand stress variation in the transfer zone is nonlinear, which is not in agreement  
578 with the ACI design code assumption. At a given location within the transfer zone, the  
579 prestress transfer to the concrete is greater than the code-predicted value. This  
580 observation posts a concern regarding concrete cracking in the transfer zone of  
581 pretensioned concrete members.

582

583 **ACKNOWLEDGEMENTS**

584 This research is supported by the University of Arkansas at Fayetteville. The authors  
585 gratefully acknowledge to several graduate researchers at the University of Arkansas in  
586 assisting with the experimental work.

587

588 **NOTATIONS**

589  $\alpha$  = exponential coefficient of bond stress-slip model

590  $A_c$  = area of concrete, mm<sup>2</sup>

591  $A_s$  = cross-sectional area of prestressing strand, mm<sup>2</sup>

592  $C_s$  = strand perimeter, mm

593  $E_c$  = concrete modulus of elasticity, MPa

594  $E_s$  = steel modulus of elasticity, MPa

595  $d_b$  = nominal strand diameter, mm

596  $F_b$  = bond magnitude

597  $f_c$  = concrete stress, MPa

598  $f'_{ci}$  = concrete compressive strength at 1 day of age, MPa

599  $f'_c$  = concrete compressive strength at 28 days of age, MPa

600  $f_s$  = strand stress, MPa

601  $f_{si}$  = initial stress, MPa

602  $f_{se}$  = effective stress, MPa

603  $f_{pu}$  = ultimate stress, MPa

604  $k_b$  = calibration coefficient

605  $L_t$  = transfer length, mm

606  $P_f$  = pullout force corresponding to free end slip of 2.5 mm (0.1 in.), kN

607  $P_i$  = pullout force corresponding to free end slip of 0.25 mm (0.01 in.), kN

608  $s(x)$  = strand slip at location  $x$

609  $s_f$  = strand slip at free end of 2.5 mm (0.1 in.)

610  $s_i$  = strand slip at free end of 0.25 mm (0.01 in.)

611  $u(x)$  = bond stress at location  $x$

612  $u_f$  = average bond stress corresponding to pullout force of  $P_f$ , MPa

613  $u_i$  = average bond stress corresponding to pullout force of  $P_i$ , MPa

614

## 615 REFERENCES

616 [1] G. Morcous, A. Hatami, M. Maguire, K. Hanna, M.K. Tadros, Mechanical and Bond  
617 Properties of 18-mm- (0.7-in.-) Diameter Prestressing Strands, *J. Mater. Civ. Eng.* 24  
618 (2012) 735–744. [https://doi.org/10.1061/\(ASCE\)MT.1943-5533.0000424](https://doi.org/10.1061/(ASCE)MT.1943-5533.0000424).

619 [2] J.K. Kim, T.R. Seong, K.P. Jang, S.H. Kwon, Tensile behavior of new 2,200 MPa and  
620 2,400 MPa strands according to various types of mono anchorage, *Struct. Eng. Mech.*  
621 47 (2013) 383–399. <https://doi.org/10.12989/SEM.2013.47.3.383>.

622 [3] J.M. Yang, H.J. Yim, J.K. Kim, Transfer length of 2400 MPa seven-wire 15.2 mm steel  
623 strands in high-strength pretensioned prestressed concrete beam, *Smart Struct. Syst.* 17  
624 (2016) 577–591. <https://doi.org/10.12989/SSS.2016.17.4.577>.

625 [4] J.S. Lawler, J.D. Connolly, A.E.N. Osborn, Acceptance Tests for Surface  
626 Characteristics of Steel Strands in Prestressed Concrete, National Academies Press,  
627 2009. <https://doi.org/10.17226/14206>.

628 [5] C.N. Dang, C.D. Murray, R.W. Floyd, W.M. Hale, J.R. Mart? -Vargas, Correlation of  
629 strand surface quality to transfer length, *ACI Struct. J.* 111 (2014).



- 630 <https://doi.org/10.14359/51686925>.
- 631 [6] V. Briere, K.A. Harries, J. Kasan, C. Hager, Dilation behavior of seven-wire  
632 prestressing strand – The Hoyer effect, *Constr. Build. Mater.* 40 (2013) 650–658.  
633 <https://doi.org/10.1016/J.CONBUILDMAT.2012.11.064>.
- 634 [7] B.W. Russell, N.H. Burns, DESIGN GUIDELINES FOR TRANSFER,  
635 DEVELOPMENT AND DEBONDING OF LARGE DIAMETER SEVEN WIRE  
636 STRANDS IN PRETENSIONED CONCRETE GIRDERS. FINAL REPORT, Austin,  
637 1993. <https://trid.trb.org/view/379831> (accessed February 19, 2022).
- 638 [8] C.D. Buckner, Review of strand development length for pretensioned concrete  
639 members, *PCI J.* 40 (1995) 84–105. <https://doi.org/10.15554/PCIJ.03011995.84.105>.
- 640 [9] J. Ramirez, B. Russell, Transfer, Development, and Splice Length for  
641 Strand/Reinforcement in High-Strength Concrete, Transportation Research Board,  
642 2008. <https://doi.org/10.17226/13916>.
- 643 [10] D. Mitchell, W.D. Cook, T. Tham, Influence of High Strength Concrete on Transfer  
644 and Development Length of Pretensioning Strand, *PCI J.* 38 (1993) 52–66.  
645 <https://doi.org/10.15554/PCIJ.05011993.52.66>.
- 646 [11] R.W. Barnes, J.W. Grove, N.H. Burns, Experimental Assessment of Factors Affecting  
647 Transfer Length, *Struct. J.* 100 (2003) 740–748. <https://doi.org/10.14359/12840>.
- 648 [12] B.H. Oh, S.N. Lim, M.K. Lee, S.W. Yoo, Analysis and Prediction of Transfer Length in  
649 Pretensioned, Prestressed Concrete Members, *Struct. J.* 111 (2014) 549–560.  
650 <https://doi.org/10.14359/51686571>.
- 651 [13] A.T. Ramirez-Garcia, R.W. Floyd, W. Micah Hale, J.R. Martí-Vargas, Influence of  
652 concrete strength on development length of prestressed concrete members, *J. Build.*  
653 *Eng.* 6 (2016) 173–183. <https://dx.doi.org/10.1016/j.jobbe.2016.03.005>.

- 654 [14] M. Arezoumandi, K.B. Looney, J.S. Volz, An experimental study on transfer length of  
655 prestressing strand in self-consolidating concrete, *Eng. Struct.* 208 (2020) 110317.  
656 <https://doi.org/10.1016/J.ENGSTRUCT.2020.110317>.
- 657 [15] M. Arezoumandi, K.B. Looney, J.S. Volz, Bond performance of prestressing strand in  
658 self-consolidating concrete, *Constr. Build. Mater.* 232 (2020) 117125.  
659 <https://doi.org/10.1016/J.CONBUILDMAT.2019.117125>.
- 660 [16] M. Arezoumandi, K.B. Looney, J.S. Volz, Development length of prestressing strand in  
661 self-consolidating concrete vs. conventional concrete: Experimental study, *J. Build.*  
662 *Eng.* 29 (2020) 101218. <https://doi.org/10.1016/J.JOBE.2020.101218>.
- 663 [17] A.A. Arab, S.S. Badie, M.T. Manzari, A methodological approach for finite element  
664 modeling of pretensioned concrete members at the release of pretensioning, *Eng.*  
665 *Struct.* 33 (2011) 1918–1929. <https://doi.org/10.1016/J.ENGSTRUCT.2011.02.028>.
- 666 [18] P. Okumus, M.G. Oliva, S. Becker, Nonlinear finite element modeling of cracking at  
667 ends of pretensioned bridge girders, *Eng. Struct.* 40 (2012) 267–275.  
668 <https://doi.org/10.1016/J.ENGSTRUCT.2012.02.033>.
- 669 [19] A.O. Abdelatif, J.S. Owen, M.F.M. Hussein, Modelling the prestress transfer in pre-  
670 tensioned concrete elements, *Finite Elem. Anal. Des.* 94 (2015) 47–63.  
671 <https://doi.org/10.1016/J.FINEL.2014.09.007>.
- 672 [20] O. Yapar, P.K. Basu, N. Nordendale, Accurate finite element modeling of pretensioned  
673 prestressed concrete beams, *Eng. Struct.* 101 (2015) 163–178.  
674 <https://doi.org/10.1016/J.ENGSTRUCT.2015.07.018>.
- 675 [21] R. Steensels, L. Vandewalle, B. Vandoren, H. Degée, A two-stage modelling approach  
676 for the analysis of the stress distribution in anchorage zones of pre-tensioned, concrete  
677 elements, *Eng. Struct.* 143 (2017) 384–397.

- 678 <https://doi.org/10.1016/J.ENGSTRUCT.2017.04.011>.
- 679 [22] K. Van Meirvenne, W. De Corte, V. Boel, L. Taerwe, Non-linear 3D finite element  
680 analysis of the anchorage zones of pretensioned concrete girders and experimental  
681 verification, *Eng. Struct.* 172 (2018) 764–779.  
682 <https://doi.org/10.1016/J.ENGSTRUCT.2018.06.065>.
- 683 [23] B.H. Oh, E.S. Kim, Y.C. Choi, Theoretical Analysis of Transfer Lengths in  
684 Pretensioned Prestressed Concrete Members, *J. Eng. Mech.* 132 (2006) 1057–1066.  
685 [https://doi.org/10.1061/\(ASCE\)0733-9399\(2006\)132:10\(1057\)](https://doi.org/10.1061/(ASCE)0733-9399(2006)132:10(1057)).
- 686 [24] J.M. Benítez, J.C. Gálvez, Bond modelling of prestressed concrete during the  
687 prestressing force release, *Mater. Struct.* 1 (2011) 263–278.  
688 <https://doi.org/10.1617/S11527-010-9625-5>.
- 689 [25] M. Markovič, N. Krauberger, M. Saje, I. Planinc, S. Bratina, Non-linear analysis of  
690 pre-tensioned concrete planar beams, *Eng. Struct.* 46 (2013) 279–293.  
691 <https://doi.org/10.1016/J.ENGSTRUCT.2012.08.004>.
- 692 [26] S.J. Han, D.H. Lee, S.H. Cho, S.B. Ka, K.S. Kim, Estimation of transfer lengths in  
693 precast pretensioned concrete members based on a modified thick-walled cylinder  
694 model, *Struct. Concr.* 17 (2016) 52–62. <https://doi.org/10.1002/SUCO.201500049>.
- 695 [27] F. Bai, J.S. Davidson, Composite beam theory for pretensioned concrete structures  
696 with solutions to transfer length and immediate prestress losses, *Eng. Struct.* 126 (2016)  
697 739–758. <https://doi.org/10.1016/J.ENGSTRUCT.2016.08.031>.
- 698 [28] C. Lee, S. Lee, S. Shin, Modeling of Transfer Region with Local Bond-Slip  
699 Relationships, *Struct. J.* 114 (2017) 187–196. <https://doi.org/10.14359/51689253>.
- 700 [29] N. Fabris, F. Faleschini, C. Pellegrino, Bond Modelling for the Assessment of  
701 Transmission Length in Prestressed-Concrete Members, *CivilEng 2020*, Vol. 1, Pages

- 702 75-92. 1 (2020) 75–92. <https://doi.org/10.3390/CIVILENG1020006>.
- 703 [30] H. Park, Z.U. Din, J.Y. Cho, Methodological Aspects in Measurement of Strand  
704 Transfer Length in Pretensioned Concrete, *Struct. J.* 109 (2012) 625–634.  
705 <https://doi.org/10.14359/51684040>.
- 706 [31] W. Zhao, B.T. Beck, R.J. Peterman, C.H.J. Wu, Development of a 5-Camera Transfer  
707 Length Measurement System for Real-Time Monitoring of Railroad Crosstie  
708 Production, 2013 Jt. Rail Conf. JRC 2013. (2013). [https://doi.org/10.1115/JRC2013-](https://doi.org/10.1115/JRC2013-2468)  
709 2468.
- 710 [32] S.J. Jeon, H. Shin, S.H. Kim, S.Y. Park, J.M. Yang, Transfer Lengths in Pretensioned  
711 Concrete Measured Using Various Sensing Technologies, *Int. J. Concr. Struct. Mater.*  
712 13 (2019) 1–16. <https://doi.org/10.1186/S40069-019-0355-Y/FIGURES/15>.
- 713 [33] ACI CODE-318-19: Building Code Requirements for Structural Concrete and  
714 Commentary, (n.d.).  
715 [https://www.concrete.org/store/productdetail.aspx?ItemID=318U19&Language=Englis](https://www.concrete.org/store/productdetail.aspx?ItemID=318U19&Language=English)  
716 h (accessed February 19, 2022).
- 717 [34] C.N. Dang, J.R. Martí-Vargas, W.M. Hale, C.N. Dang, J.R. Martí-Vargas, W.M. Hale,  
718 *Structural Engineering and Mechanics*, *Struct. Eng. Mech.* 76 (2020) 67.  
719 <https://doi.org/10.12989/SEM.2020.76.1.067>.
- 720 [35] American Association of State Highway and Transportation Officials, AASHTO LRFD  
721 Bridge Design Specifications, 9th Edition, 2020. <https://trid.trb.org/view/1704698>  
722 (accessed February 19, 2022).
- 723 [36] G. Morcous, S. Assad, A. Hatami, M.K. Tadros, Implementation of 0.7 in. diameter  
724 strands at  $2.0 \times 2.0$  in. spacing in pretensioned Bridge girders, *PCI J.* 59 (2014) 145–  
725 158. <https://doi.org/10.15554/PCIJ.06012014.145.158>.

- 726 [37] G. Schuler, Producer's Experience with 10,000 psi Concrete and 0.7-in. Diameter  
727 Strands - Concrete Bridge Views, *Concr. Bridg. Views*. 54 (2009) 9–11.  
728 [http://concretebridgeviews.com/2009/03/producers-experience-with-10000-psi-](http://concretebridgeviews.com/2009/03/producers-experience-with-10000-psi-concrete-and-0-7-in-diameter-strands/)  
729 [concrete-and-0-7-in-diameter-strands/](http://concretebridgeviews.com/2009/03/producers-experience-with-10000-psi-concrete-and-0-7-in-diameter-strands/) (accessed February 19, 2022).
- 730 [38] ASTM A1081/A1081M-21, Standard Test Method for Evaluating Bond of Seven-Wire  
731 Steel Prestressing Strand, West Conshohocken, 2021.  
732 [https://www.astm.org/a1081\\_a1081m-21.html](https://www.astm.org/a1081_a1081m-21.html) (accessed February 19, 2022).
- 733 [39] G.L. Balazs, Transfer Control of Prestressing Strands, *PCI J.* 37 (1992) 60–71.  
734 <https://doi.org/10.15554/PCIJ.11011992.60.71>.
- 735 [40] J.A. den Uijl, Bond Modelling of Prestressing Strand, *Spec. Publ.* 180 (1998) 145–170.  
736 <https://doi.org/10.14359/5876>.
- 737 [41] H. Park, J.Y. Cho, Bond-Slip-Strain Relationship in Transfer Zone of Pretensioned  
738 Concrete Elements, *Struct. J.* 111 (2014) 503–514. <https://doi.org/10.14359/51686567>.
- 739 [42] J.R. Martí-Vargas, W.M. Hale, E. García-Taengua, P. Serna, Slip distribution model  
740 along the anchorage length of prestressing strands, *Eng. Struct.* 59 (2014) 674–685.  
741 <https://doi.org/10.1016/J.ENGSTRUCT.2013.11.032>.
- 742 [43] C.N. Dang, R.W. Floyd, C.D. Murray, W.M. Hale, J.R. Martí-Vargas, Bond stress-slip  
743 model for 0.6 in. (15.2 mm) diameter strand, *ACI Struct. J.* 112 (2015).  
744 <https://doi.org/10.14359/51687750>.
- 745 [44] R.S. Kareem, A. Al-Mohammedi, C.N. Dang, C.N. Dang, J.R. Martí-Vargas, W.M.  
746 Hale, Bond model of 15.2 mm strand with consideration of concrete creep and  
747 shrinkage, <https://doi.org/10.1680/Jmacr.18.00506>. 72 (2020) 799–810.  
748 <https://doi.org/10.1680/JMACR.18.00506>.
- 749 [45] A. Pozolo, B. Andrawes, Analytical prediction of transfer length in prestressed self-

- 750 consolidating concrete girders using pull-out test results, *Constr. Build. Mater.* 25  
751 (2011) 1026–1036. <https://doi.org/10.1016/J.CONBUILDMAT.2010.06.076>.
- 752 [46] M. Tadros, G. Morcous, Impact of Large 0.7 Inch Strand on NU-I Girders, Lincoln,  
753 NE, 2011. <https://digitalcommons.unl.edu/matcreports/48> (accessed February 19,  
754 2022).
- 755 [47] C. Dang, Measurement of Transfer and Development Lengths of 0.7 in. Strands on  
756 Pretensioned Concrete Elements, University of Arkansas, 2015.  
757 <https://scholarworks.uark.edu/etd/1076> (accessed February 19, 2022).
- 758 [48] K.H. Khayat, D. Mitchell, Self-Consolidating Concrete for Precast, Prestressed  
759 Concrete Bridge Elements, National Academies Press, Washington, DC, 2009.  
760 <https://doi.org/10.17226/14188>.
- 761 [49] B.W. Russell, N.H. Bums, Measured transfer lengths of 0.5 and 0.6 in. Strands in  
762 pretensioned concrete, *PCI J.* 41 (1996) 44–64.  
763 <https://doi.org/10.15554/PCIJ.09011996.44.65>.
- 764 [50] C.N. Dang, W.M. Hale, J.R. Martí-Vargas, Assessment of transmission length of  
765 prestressing strands according to fib Model Code 2010, *Eng. Struct.* 147 (2017).  
766 <https://doi.org/10.1016/j.engstruct.2017.06.019>.
- 767 [51] M. Tadros, G. Morcous, Impact of 0.7 inch Diameter Strands on NU I-Grinders,  
768 Lincoln, NE, 2011. <https://digitalcommons.unl.edu/ndor/88> (accessed February 19,  
769 2022).
- 770 [52] Q. Patzlaff, G. Morcous, K. Hanna, M.K. Tadros, Bottom Flange Confinement  
771 Reinforcement in Precast Prestressed Concrete Bridge Girders, *J. Bridg. Eng.* 17 (2012)  
772 607–616. [https://doi.org/10.1061/\(ASCE\)BE.1943-5592.0000287](https://doi.org/10.1061/(ASCE)BE.1943-5592.0000287).
- 773 [53] M. Maguire, G. Morcous, M.K. Tadros, Structural Performance of Precast/Prestressed

774 Bridge Double-Tee Girders Made of High-Strength Concrete, Welded Wire  
775 Reinforcement, and 18-mm-Diameter Strands, *J. Bridg. Eng.* 18 (2013) 1053–1061.  
776 [https://doi.org/10.1061/\(ASCE\)BE.1943-5592.0000458](https://doi.org/10.1061/(ASCE)BE.1943-5592.0000458).

777 [54] W. Song, Z.J. Ma, J. Vadivelu, E.G. Burdette, Transfer Length and Splitting Force  
778 Calculation for Pretensioned Concrete Girders with High-Capacity Strands, *J. Bridg.*  
779 *Eng.* 19 (2014) 04014026. [https://doi.org/10.1061/\(ASCE\)BE.1943-5592.0000566](https://doi.org/10.1061/(ASCE)BE.1943-5592.0000566).

780 [55] J. Salazar, H. Yousefpour, R.A. Abyaneh, H. Kim, A. Katz, T. Hrynyk, O. Bayrak, End-  
781 Region Behavior of Pretensioned I-Girders Employing 0.7 in. (17.8 mm) Strands,  
782 *Struct. J.* 115 (2018) 91–102. <https://doi.org/10.14359/51700783>.

783 [56] C.N. Dang, W.M. Hale, R.W. Floyd, J.R. Martí-Vargas, Prediction of development  
784 length from free-end slip in pretensioned concrete members, *Mag. Concr. Res.* 70  
785 (2018). <https://doi.org/10.1680/jmacr.17.00334>.

786 [57] Precast-Prestressed Concrete Institute, *PCI Design Handbook*, 2017.  
787 <https://www.pci.org/ItemDetail?iProductCode=MNL-120-17#1> (accessed February 20,  
788 2022).

789 [58] L.A. Caro, J.R. Martí-Vargas, P. Serna, Time-dependent evolution of strand transfer  
790 length in pretensioned prestressed concrete members, *Mech. Time-Dependent Mater.* 4  
791 (2013) 501–527. <https://doi.org/10.1007/S11043-012-9200-2>.

792 [59] L. Chen, B.A. Graybeal, Modeling Structural Performance of Second-Generation  
793 Ultrahigh-Performance Concrete Pi-Girders, *J. Bridg. Eng.* 17 (2012) 634–643.  
794 [https://doi.org/10.1061/\(ASCE\)BE.1943-5592.0000301](https://doi.org/10.1061/(ASCE)BE.1943-5592.0000301).

795 [60] G. Zhang, B.A. Graybeal, Development of UHPC Pi-Girder Sections for Span Length  
796 up to 41 m, *J. Bridg. Eng.* 20 (2015) 04014068.  
797 [https://doi.org/10.1061/\(ASCE\)BE.1943-5592.0000653](https://doi.org/10.1061/(ASCE)BE.1943-5592.0000653).

- 798 [61] C.D. Murray, M. Diaz Arancibia, P. Okumus, R.W. Floyd, Destructive testing and  
799 computer modeling of a scale prestressed concrete I-girder bridge, *Eng. Struct.* 183  
800 (2019) 195–205. <https://doi.org/10.1016/J.ENGSTRUCT.2019.01.018>.
- 801 [62] C.N. Dang, R.W. Floyd, W.M. Hale, J.R. Martí-Vargas, Spacing requirements of 0.7 in.  
802 (18 mm) diameter prestressing strands, *PCI J.* 61 (2016).  
803 <https://doi.org/10.15554/pcij.01012016.70-87>.
- 804 [63] K. Warenycia, M. Diaz-Arancibia, P. Okumus, Effects of confinement and concrete  
805 nonlinearity on transfer length of prestress in concrete, *Structures.* 11 (2017) 11–21.  
806 <https://doi.org/10.1016/J.ISTRUC.2017.04.002>.
- 807